

Trapping effects in *a*-Si:H investigated by small-signal transient photoconductivity and the steady-state photocarrier-grating technique

M. Haridim, M. Zelikson, and K. Weiser

Department of Electrical Engineering and Solid State Institute, Technion, Haifa, Israel

(Received 27 May 1993; revised manuscript received 20 December 1993)

We report on trapping effects observed in small-signal photoconductivity and steady-state photocarrier-grating (SSPG) experiments. In the former case trapping effects appear since the small-signal photocurrent decays exponentially with time after the excitation is turned off, but with a decay time which depends on the ratio of free to trapped carriers and is determined by the intensity of the cw background illumination. In the case of (steady-state) SSPG measurements, carried out as a function of electric field, an electron drift mobility is obtained which is proportional to the ratio of free to trapped carriers and is therefore again determined by the background illumination. Both experiments show that around 0.4 eV below the electron mobility edge the density of states falls off much more slowly with energy towards midgap than near the mobility edge and may even exhibit a minimum.

I. INTRODUCTION

The importance of traps for many transport and recombination phenomena which occur in amorphous semiconductors is well known. Indeed, the existence of a continuum of traps close to the mobility edges is one of the features which distinguishes amorphous from crystalline semiconductors, where such traps, if present at all, exist only at discrete energy levels within the forbidden gap. A prime example of a trap-controlled phenomenon is the fact that time-of-flight experiments¹ do not yield the mobility of free carriers but, rather, a "drift" mobility which is lower because carriers are trapped and reemitted continuously during their transit through the sample. (We state at the outset that we use the word "trap" in the sense of a localized state which, when occupied by an electron or hole, reemits the particle mainly to the band from which it originates rather than permitting it to combine with a carrier of opposite sign, as would be the case for a recombination center.^{2,3})

In this paper we show that trapping phenomena can be studied more quantitatively by the use of small-signal transient photoconductivity, or by steady-state photocarrier-grating (SSPG) experiments,^{4,5} than by time-of-flight experiments. In both cases a strong background beam illuminates the sample, and a much weaker signal beam is superimposed on it. In the case of transient photoconductivity experiments the weak signal beam is turned off after the system has reached a steady state, and the current produced by it during its decay is monitored. In the case of the SSPG method the experimental conditions are chosen to either allow or disallow interference between the two beams, and the photocurrent produced by the weak beam is measured under these two conditions. Thus both experiments discussed in this paper involve a strong background beam and a weak signal beam. In the case of the transient photoconductivity experiment the role of traps is obvious. As discussed in detail below, the presence of a strong background beam controls the number of localized states

which act as traps for the carriers produced by the weak excitation beam. Since during the decay of the photocurrent free electrons are replenished from the reservoir of the electrons which had been trapped during the steady-state part of the weak excitation, the decay time reflects these trapping effects. The role of traps in SSPG experiments is less obvious, since they are carried out under steady-state conditions. They arise from the fact that carriers do not recombine in the same place where they are created, because of diffusion and drift in electric fields.

The analysis of the transient photocurrent and the SSPG experiments described in this paper yields the result that the density of states near the electron quasi-Fermi level at about 0.4 eV below the electron mobility edge falls off much more slowly with energy toward midgap than near the mobility edge, or that a minimum in the density of states exists at that energy.

II. EXPERIMENTAL PROCEDURE

The three samples investigated in this work were undoped *a*-Si:H films, typically 1 μm thick, produced by rf decomposition of silane on quartz substrates. The samples had dark conductivities between 4 and $5 \times 10^{-12} \Omega^{-1} \text{cm}^{-1}$, and the dark Fermi levels were typically 0.75 eV below the mobility edge.⁶

Before the start of the measurements the samples were intentionally "degraded" (Ref. 7) by exposing them to light with an intensity of about 100 mW/cm² for 10 h. A He-Ne laser ($\lambda = 0.6328 \mu\text{m}$) was used both for the SSPG measurements^{4,5} and for the transient photocurrent experiments. In the latter case the laser beam passed through an acousto-optic modulator with a rise-and-fall time of 20 ns which periodically reduced the intensity by 5%. In this manner, a small-signal excitation pulse was superimposed on the background optical bias. The photocurrent was measured vs time during its decay from its steady value, using a circuit whose response time was much shorter than any decay times measured. The exci-

tation pulses were 20 μ s long in order to make certain that the photocarriers created during its duration had a chance to come to a dynamic equilibrium among themselves and the background photocarriers.⁸ The experimental results described below were reproducible from sample to sample.

III. EXPERIMENTAL RESULTS

A. Photocurrent decay

In Fig. 1 we show some decay curves of the incremental photocurrent for a number of optical biases. Clearly, at high background light intensities the current decays exponentially with time so that a "lifetime" τ can be defined. This lifetime increases with lower optical bias, but below around 1 mW/cm^2 one can no longer be certain of an exponential decay since it was measured over less than one order of magnitude. The lifetimes obtained from Fig. 1 are plotted against the background light intensity, as well as against the conductivity corresponding to it, in Fig. 2. The plot vs conductivity is presented since it is more significant for the interpretation of the data than the plot vs intensity, as is shown below. The conductivity was calculated from the measured sample conductance by taking the effective thickness of the sample as α^{-1} , where α is the absorption constant for He-Ne light.⁹ A number of small-signal, two-beam experiments have been reported in the literature.¹⁰⁻¹⁵ With the exception of Ref. 10, however, none covered as extensive a range of background illuminations as the work reported here, in which lifetimes in the submicrosecond range were measured. Comparing the results obtained here to those reported in Ref. 10 for similar experiments, we find that our decay times are approximately 20 times shorter than those in Ref. 10 at comparable light intensities. However, since in the latter case both fast and slow components were observed in the decay curves, it is difficult to deduce a simple lifetime from those data. We believe that this difference in behavior stems from the fact that long excitation pulses were used by us for reasons stated at the end of Sec. II. By contrast, the use of short excitation pulses in Ref. 10 means that both thermalization and recombination processes occurred during the decay.

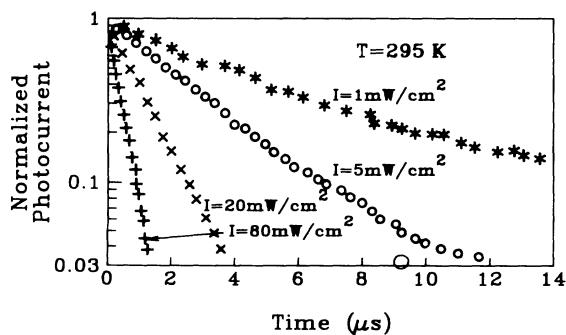


FIG. 1. Normalized photocurrent vs time during decay of small-signal photocurrent. Measurements at room temperature.

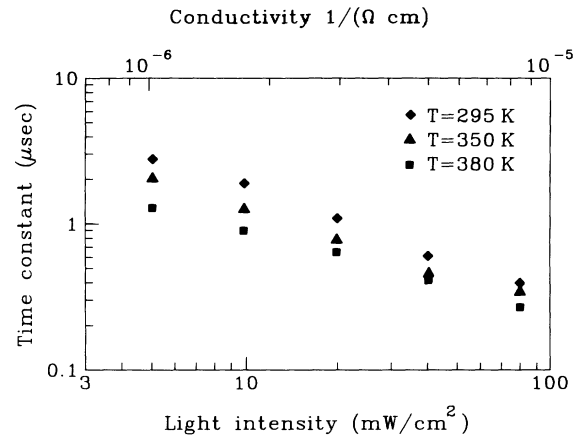


FIG. 2. Time constants derived from exponential parts of photocurrent decay curves (Fig. 1) vs light intensity of background beam and vs conductivity of sample.

B. SSPG Results

In Fig. 3 we show the results of SSPG measurements at a grating wavelength of 6 μ m, at different electric fields E , and at three different light intensities I of the background beam. The symbol $\Delta\sigma_{\parallel}(E)$ denotes the difference between the small-signal photoconductivities under interference and noninterference conditions^{16,17} at a given E . Along the ordinate of Fig. 3 the values of $\Delta\sigma_{\parallel}(E)$ are normalized to $\Delta\sigma_{\parallel}(0)$ at negligible electric fields where the ordinate approaches a constant value.^{11,16,17} As E increases, the ratio $\Delta\sigma_{\parallel}(E)/\Delta\sigma_{\parallel}(0)$ decreases, since an electric field tends to smear out the effect of the modulation of the sample conductance by the interference, in much the same manner as diffusion does.^{11,16,17} This effect is further discussed in Sec. IV B.

IV. DISCUSSION

A. Small-signal photocurrent decay

We first discuss the lifetime results embodied in Figs. 1 and 2. The idea of monitoring the decay of the current produced by a weak beam, while continuously illuminat-

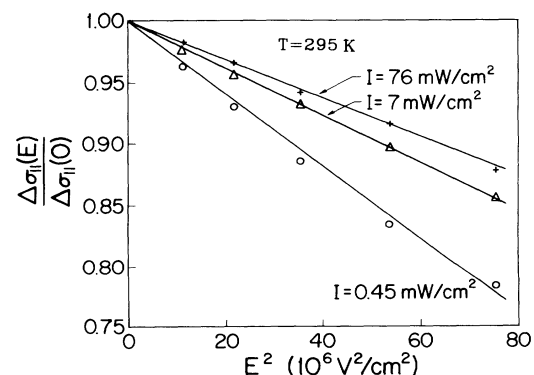


FIG. 3. Dependence of normalized interference photoconductivity vs square of the electric field at different background light intensities I . See text for definitions of $\Delta\sigma_{\parallel}(E)$ and $\Delta\sigma_{\parallel}(0)$. Measurements at room temperature.

ing the sample with a strong beam, is not new.^{11,12,18} The main idea is to keep the position of the trapped electron and hole quasi-Fermi levels³ constant both during the steady-state part of the weak excitation and during its decay. This constancy is achieved by using a background beam which is much more intense than the signal beam. In this manner, the recombination probability of carriers remains constant throughout the experiment, since it is determined by the recombination traffic through states between the quasi-Fermi levels.³ Since the recombination probability remains constant during the decay of the photocurrent, the influence of electron trapping on the decay kinetics can now be investigated. These trapped electrons "slow down" the decay of the photocurrent, since they are continuously released into the conduction band after the excitation is turned off. Such a two-beam, small-signal experiment, in which the quasi-Fermi levels are kept constant, are clearly easier to interpret than conventional, single-beam transient photoconductivity experiments.¹⁹ In particular, as shown experimentally in Fig. 1 and as will be discussed below, exponential decay curves can be obtained if the background illumination is strong enough so that the electron quasi-Fermi level is "sufficiently close" to the mobility edge. Such exponential decay curves can be obtained only in a two-beam experiment, such as described in this paper. Without the background beam the quasi-Fermi level moves continuously downward toward the dark Fermi level during the decay of the photocurrent, and nonexponential decay curves are observed.

Since this paper is concerned only with trapping effects, we do not discuss the recombination process itself such as the kinetics of recombination via dangling bonds.^{20,21} We merely assume that at the beginning of the recombination process either the electron or the hole starts off in an extended state, and hence we neglect the recombination between localized electrons and holes.

We first calculate the ratio of trapped to free electrons produced by the weak excitation in the steady state, i.e., before the excitation is turned off. We shall refer to these electrons as "excess" electrons in order to distinguish them from those produced by the background beam. Electrons present in thermal equilibrium can be neglected since the photoconductivity is several orders of magnitude greater than the dark conductivity. The distribution function for photoelectrons in a state with energy ϵ between the mobility edge and the intrinsic Fermi level ϵ_{F0} is given by a modified Fermi-Dirac function:³

$$f(\epsilon) = \frac{[Rn/(Rn+p)]}{1 + \exp(\epsilon - \epsilon_{ft}/kT)}. \quad (1)$$

In this equation n and p are concentrations of free photoelectrons and holes, respectively, and R is the ratio of the capture cross sections for electrons and holes by a localized state in this energy range. ϵ_{ft} is a "trapped electron Fermi level," closely related to a "demarcation level" (Ref. 2) above which an excess electron is likely to be reemitted to the conduction band, and below which it is likely to recombine with a hole. We assume throughout this paper that $n \gg p$,²¹ so that unless R is very small the factor $Rn/(Rn+p)$ is close to unity. Hence, the distri-

bution function of Eq. (1) is very similar to an ordinary Fermi-Dirac function, and to a very good approximation the characteristic energy ϵ_{ft} can be replaced by the quasi-Fermi level for electrons, ϵ_q .²¹ This level is defined by the relation $n = N_c/[1 + \exp(-\epsilon_q/kT)]$, where N_c is a concentration of thermally accessible states above the mobility edge which is taken as the zero of energy.

Replacing ϵ_{ft} in Eq. (1) by ϵ_q above, we write the ratio of trapped to free excess carriers as

$$\left(\frac{\Delta n_t}{\Delta n_s} \right)_0 = \frac{\int_{\epsilon_{f0}}^0 g(\epsilon)[f(\epsilon, \epsilon_q + \delta\epsilon_q) - f(\epsilon, \epsilon_q)]d\epsilon}{N_c[\exp(\epsilon_q + \delta\epsilon_q)/KT - \exp\epsilon_q/KT]}. \quad (2)$$

Here ϵ_q is the quasi-Fermi level determined by the background illumination, and $\delta\epsilon_q$ is the increase in the quasi-Fermi level by the weak excitation. $g(\epsilon)$ is the density-of-states function, and $f(\epsilon)$ the Fermi-Dirac function. Since ϵ_{f0} , the intrinsic Fermi level,³ is many times kT below the mobility edge, the lower limit in the integral of Eq. (2) can be replaced by minus infinity. To evaluate the integral one must still know the distribution function $g(\epsilon)$, but since most of the excess electrons will be trapped near the quasi-Fermi level ϵ_q , it is only necessary to know $g(\epsilon)$ near it. We postulate that $g(\epsilon) = g(\epsilon_q)\exp(\alpha\epsilon_q/kT)$, with α equal to T/T_0 .

We stress the point that KT_0 is the falloff parameter of $g(\epsilon)$ near ϵ_q which, as we shall see below, is different from that measured near the mobility edge. Introducing this expression into Eq. (2), we obtain

$$\left(\frac{\Delta n_t}{\Delta n_s} \right)_0 = \frac{\pi\alpha}{\sin\pi\alpha} \frac{KTg(\epsilon_q)}{N_c} \exp\{(\alpha-1)\epsilon_q/KT\}. \quad (3)$$

Equation (3) is valid even if T_0 varies between ϵ_q and ϵ_c , since most of the contribution to the integral comes from states near ϵ_q .

We now turn to the transient results, which show that if the background light intensity is high enough, i.e., ϵ_q is close to ϵ_c , the photocurrent decay curves are exponential. We define ϵ_q^* as that value of ϵ_q above which an exponential decay is observed over more than a decade, namely, for $I \approx 5$ mW/cm², or $\sigma = 1 \times 10^{-6}$ Ω^{-1} cm⁻¹. Relative to the dark Fermi level ϵ_f , the quasi-Fermi-level ϵ_q is given by $\epsilon_q = \epsilon_f + KT \ln[\sigma(I)/\sigma_{\text{dark}}]$ so that $\epsilon_q^* = -0.43$ eV at 300°K. Over the range of ϵ_q 's from -0.43 to -0.37 eV, at 80 mW/cm² or $\sigma = 1 \times 10^{-5}$ Ω^{-1} cm⁻¹, meaningful lifetimes could thus be measured, with values shown in Fig. 2. We now show that such an exponential decay demands that $(\Delta n_t/\Delta n_s)_0$ remains constant during the decay. The rate equation for the free electrons can be written as

$$\frac{d}{dt} n_f(t) = -\frac{n_f}{\tau_f} - \int_{-\infty}^0 \frac{d}{dt} n_t(\epsilon, t) d\epsilon + G_0, \quad (4)$$

where τ_f is the free-electron lifetime, and the justification for using minus infinity as the lower limit of the integral was given earlier. Since we observe an exponential decay for Δn , we substitute $\Delta n_f(0)\exp(-t/\tau)$ into Eq. (4), which

can then be written as

$$\frac{d}{dt} \Delta n_{\text{tot}} = -\frac{\Delta n_f(0)}{\tau_f} \exp\left[-\frac{t}{\tau}\right], \quad (5)$$

where $\Delta n_{\text{tot}} = \Delta n_f(t) + \int_{-\infty}^0 \Delta n_t(\varepsilon) d\varepsilon$. The solution of Eq. (5) yields an effective lifetime τ :

$$\tau = \tau_f \left[\frac{\Delta n_{\text{tot}}}{\Delta n_f} \right]_0 \approx \tau_f \frac{\Delta n_t}{\Delta n_f}. \quad (6)$$

Equation (6) postulates that the ratio of trapped-to-free electrons during the exponential part of the decay remains the same as that before the light pulse is turned off, and that $\tau \gg \tau_f$. Substituting Eq. (3) into Eq. (6), one obtains

$$\tau = \tau_f \frac{\pi\alpha}{\sin\pi\alpha} \frac{KT}{N_C} g_0 \exp\left\{(\alpha-1) \frac{\varepsilon_q}{KT}\right\}. \quad (7)$$

In order to compare this relation to experimental results we use $n = N_C \exp(\varepsilon_q/KT)$ and $n = \kappa I \tau_f(I)$, where κ is the absorption coefficient; Eq. (7) can now be rewritten in the form

$$\tau = [\tau_f(I)]^\alpha \frac{\pi\alpha}{\sin\pi\alpha} \frac{KTg_0}{N_C} \left[\frac{\kappa}{N_C} \right]^{\alpha-1} I^{\alpha-1}. \quad (8)$$

Since from steady-state measurements (Fig. 4) we find that $\sigma \propto I^\gamma$, the free-carrier lifetime is proportional to $I^{\gamma-1}$. The final relation between τ and I then becomes

$$\log_{10} \tau = \left[\gamma \frac{T}{T_0} - 1 \right] \log_{10} I + \text{const}, \quad (9)$$

where $\gamma = 0.85$ and is independent of temperature. Experimentally, a linear relation between $\ln \tau$ and $\ln I$ is indeed seen in Fig. 2, so that one should be able to calculate T_0 from the dependence of the slopes at different temperatures. The scatter in the data is too great, however, to determine T_0 with much reliability in this manner. By taking an average of the slopes at a mean temperature of 340°K one finds $T_0 = 930 \pm 100$ K. We shall discuss this result further below, but first turn our attention to the physical origin of the dependence of τ on I , or σ , and to the conditions under which Eq. (7) is valid.

The reason τ decreases with increasing background illumination is readily understood from Eq. (3), which shows that the ratio of trapped to free carriers decreases as ε_q approaches ε_c . Hence, as free carriers start to recombine following the end of the excitation pulse they are replenished by a smaller number of trapped carriers the closer ε_q is to ε_c . Since it is the replenishment of free carriers by trapped carriers which slows up the decay of the photoconductivity, τ decreases as $\varepsilon_q \rightarrow \varepsilon_c$.

The above picture, in which the ratio of free-to-trapped carriers remains constant during the decay, i.e., the ensemble of excess carriers decays with a single lifetime given by (7), breaks down if ε_q is too far away from ε_c . Clearly, in order for the model to be valid the release time for carriers trapped near ε_q must be shorter than, or

at least equal to, the ensemble lifetime τ :

$$\nu_0^{-1} \exp\{(\varepsilon_c - \varepsilon_q)/KT\} \leq \tau, \quad (10)$$

where ν_0 is an attempt-to-escape frequency. As stated in Sec. III A, well-defined exponential decay curves were obtained for $I > 5$ mW/cm², corresponding to a sample conductivity of 1×10^{-6} ($\Omega \text{ cm}$)⁻¹ or a quasi-Fermi level 0.43 eV below the mobility edge. The measured lifetime at that intensity was 2.5 μs . Inserting these values into (10) one obtains $\nu_0 = 6 \times 10^{12}$ s⁻¹, which is a very reasonable value for an optical-phonon frequency.

B. SSPG measurements at high electric fields

SSPG measurements at negligible electric fields, E , yield the ambipolar diffusion length L of the photocarriers which is dominated by the carriers with the smaller drift mobility, presumably the holes.^{4,5} If, on the other hand, these measurements are extended to fields which are substantially greater than KT/qL , information about the drift mobility of the majority carriers can also be obtained. This conclusion is readily reached by considering the theoretically predicted¹⁷ dependence on E of the ratio of the small-signal photoconductivities, $\Delta\sigma_{\parallel}(E)/\Delta\sigma_{\parallel}(0)$, which were defined in Sec. III B. To second order in E ,

$$\frac{\Delta\sigma_{\parallel}(E)}{\Delta\sigma_{\parallel}(0)} = 1 - \frac{k^2 \mu_n \mu_p \tau^2}{a} E^2. \quad (11a)$$

The new symbols appearing above are the grating wave vector k , the small signal drift mobilities of electrons and holes μ_n and μ_p , and the factor a which is the ratio of the lifetime to the dielectric relaxation time τ_{rel} . Writing τ_{rel} as ε/σ , where ε is the permittivity of the material, Eq. (11a) can be rewritten as

$$\frac{\Delta\sigma_{\parallel}(E)}{\Delta\sigma_{\parallel}(0)} = 1 - \frac{\varepsilon k^2 \mu_n \mu_p \tau}{\sigma} E^2. \quad (11b)$$

We now assume that the ambipolar diffusion length obtained from the SSPG data can be set equal to $\sqrt{D_p \tau}$ so that, using the Einstein relation, $\mu_p \tau$ in Eq. (11b) can be replaced by $L^2/(KT/q)$. The small-signal drift mobility

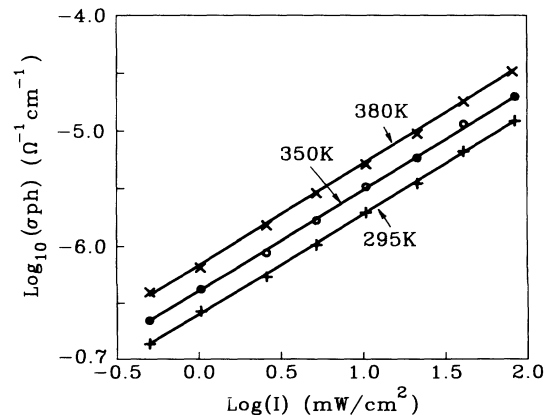


FIG. 4. Steady-state photoconductivity of sample vs background illumination (mW/cm²).

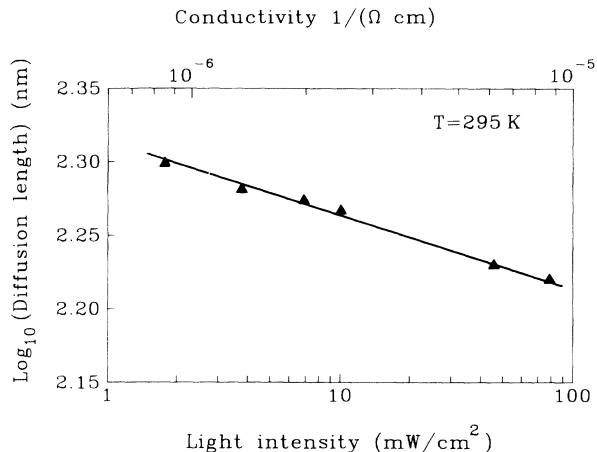


FIG. 5. Ambipolar diffusion length vs light intensity of background beam and vs sample conductivity. Measurements at room temperature.

of electrons μ_n can then be calculated from the slopes of the curves of Fig. 3 using the values of L at different light intensities, which are shown in Fig. 5. The results for μ_n are displayed in column 3 of Table I.

The first point to be made about these values of μ_n is that they are much lower than electron drift mobilities obtained from time-of-flight (TOF) experiments.¹ The difference reflects the fact that in these steady-state measurements free electrons interact mainly with states clustered near the quasi-Fermi level at about 0.4 eV below the mobility edge. By contrast, in TOF experiments much shallower trap states determine the drift mobilities.²¹

The second point of interest concerns the strong dependence of the drift mobility on the conductivity of the sample or, equivalently, on the position of the quasi-Fermi level. The reason for this strong dependence is that, as discussed above, trapping effects become less pronounced as ϵ_q approaches ϵ_c . Setting the drift mobility equal to $\mu_n^0 \Delta n_f / \Delta n_t$, where μ_n^0 is the free-carrier mobility, and using Eq. (3), the relation between μ_n and ϵ_q becomes

$$\mu_n = \mu_n^0 \frac{N_c}{KTg_0} \frac{\sin \pi \alpha}{\pi \alpha} \exp \left\{ (1 - \alpha) \frac{\epsilon_q}{KT} \right\}. \quad (12)$$

Since the photoconductivity is proportional to $\exp(\epsilon_q/KT)$, a plot of $\ln \mu$ vs σ , with μ taken from column 3 of Table I, should have a slope of $1 - \alpha$, from which α can then be obtained. We do not present such a plot in this paper since its slope is essentially unity, as seen from a visual inspection of columns 2 and 3 of Table I. More precisely, the slope of such a graph is 0.96 ± 0.02 , so that α is approximately 0.04, in contrast to the results of the transient photoconductivity measurements which yielded $\alpha = 0.32$. Thus the latter measurements suggest that the density of states near 0.4 eV below the mobility edge falls off much more slowly than near the mobility edge, where α at room temperature is ~ 0.7 (Ref. 22) or even close to unity (Ref. 23). The SSPG results, on the other hand, actually suggest a minimum in the density of states, as reported near -0.4 eV from photoelectron

TABLE I. Small-signal drift mobility μ_n at three different background light intensities I and sample conductivities σ .

I (mW/cm ²)	σ (1/Ω cm)	μ_n (cm ² /V s)
76	1.0×10^{-5}	1.3×10^{-2}
7	1.3×10^{-6}	2.0×10^{-3}
0.45	1.0×10^{-7}	1.6×10^{-4}

spectroscopy.²² The reason for the difference between the α 's obtained by the two measurement techniques used in this paper is not clear.

V. CONCLUSIONS

In this paper we have combined two seemingly disparate experiments which throw light on trapping phenomena in amorphous semiconductors. Trapping effects manifest themselves in the case of transient photoconductivity in a rather obvious manner: they give rise to the power-law dependence of the decay of photoconductivity on time when measured on a sample without background illumination. In the present small-signal experiments, on the other hand, an exponential decay with time is observed, provided the background light intensity is high enough. The "lifetime" of the incremental photocarriers thus determined depends strongly on trapping effects, since carriers which in the steady state were trapped are released as the free carriers recombine. This release rate depends on the background illumination.

In SSPG experiments trapping effects manifest themselves in a somewhat less obvious fashion than in transient photoconductivity experiments. In this case trapping effects are due to the fact that the sample is not uniformly illuminated, and hence drift mobilities of free and trapped photocarriers created by the weak beam rather than the mobility of only the free carriers enter into the diffusion and drift lengths measured by the SSPG technique. As in the case of the transient photoconductivity experiments, the background illumination controls the trapping effects which, in turn, affect the drift mobilities.

While both experiments clearly illustrate these trapping effects, they yield different values for the logarithmic slope of the density of states vs energy at an energy of about 0.4 eV below the mobility edge of the electrons. Transient photoconductivity measurements suggest that this slope merely falls off by a factor of 3 at that energy, compared to its value near the mobility edge. The SSPG results, on the other hand, suggest that an actual minimum exists in the density of states at that energy. The reason for the difference in the results is not clear, and it is evident that either more experimental work along these lines is needed or that the theories underlying the present work need to be refined.

ACKNOWLEDGMENTS

We thank S. Cohen for excellent help in carrying out these experiments, Dr. H. Mell for supplying the samples used and Dr. S. Baranovski for valuable discussions, particularly in connection with Eq. (10). This work was carried out under the sponsorship of Kernforschungsanlage Julich and the Israeli National Research Council.

- ¹W. E. Spear, in *Advances in Disordered Semiconductors*, edited by H. Fritzsche (World Scientific, Singapore, 1989), Vol. I.
- ²A. Rose, *Concepts in Photoconductivity and Allied Problems* (Wiley-Interscience, New York, 1963).
- ³J. C. Simmons and G. W. Taylor, *Phys. Rev. B* **4**, 502 (1971).
- ⁴D. Ritter, E. Zeldov, and K. Weiser, *Appl. Phys. Lett.* **49**, 791 (1986).
- ⁵D. Ritter, K. Weiser, and E. Zeldov, *J. Appl. Phys.* **62**, 4563 (1987).
- ⁶H. Mell and X. Marburg (private communication).
- ⁷D. L. Staebler and C. R. Wronski, *Appl. Phys. Lett.* **31**, 292 (1977).
- ⁸E. Zeldov and K. Weiser, *Solid State Commun.* **67**, 903 (1988).
- ⁹G. D. Cody in *Semiconductors and Semimetals*, edited by J. Pankove (Academic, New York, 1984), Vol. 21B.
- ¹⁰Xing Chen and C. Tai, *Phys. Rev. B* **40**, 9652 (1989).
- ¹¹D. Ritter, E. Zeldov, and K. Weiser, *Phys. Rev. B* **38**, 8296 (1988).
- ¹²R. Pandya and E. A. Schiff, *Philos. Mag.* **52**, 1075 (1985).
- ¹³K. A. Conrad, R. Pandya, and E. A. Schiff, *Phys. Rev. Lett.* **54**, 247 (1985).
- ¹⁴P. Tzanetakas, H. Mell, and W. Fuhs, *J. Non-Cryst. Solids* **137/138**, 465 (1991).
- ¹⁵F. Wang *et al.*, *J. Non-Cryst. Solids* **137/138**, 511 (1991).
- ¹⁶D. Ritter and K. Weiser, *Phys. Rev. B* **34**, 9031 (1986).
- ¹⁷Y. M. Li, *Phys. Rev. B* **42**, 9025 (1990).
- ¹⁸E. Zeldov and K. Weiser, *Phys. Rev. Lett.* **53**, 1012 (1984).
- ¹⁹C. R. Wronski and R. E. Daniel, *Phys. Rev. B* **23**, 794 (1981).
- ²⁰E. Sauvain, J. Hubin, A. Shah, and P. Pipoz, *Philos. Mag. B* **63**, 327 (1991).
- ²¹J. Kocka, C. E. Nebel, and C. D. Abel, *Philos. Mag.* **63**, 221 (1991).
- ²²K. Winer and L. Ley, *Advances in Disordered Semiconductors*, edited by H. Fritsch (World Scientific, Singapore, 1989), Fig. 9, p. 383.
- ²³T. Tiedje, J. M. Cebulka, D. L. More, and B. Abeles, *Phys. Rev. Lett.* **46**, 1425 (1981).